

(This is a sample cover image for this issue. The actual cover is not yet available at this time.)

This article appeared in a journal published by Elsevier. The attached copy is furnished to the author for internal non-commercial research and education use, including for instruction at the authors institution and sharing with colleagues.

Other uses, including reproduction and distribution, or selling or licensing copies, or posting to personal, institutional or third party websites are prohibited.

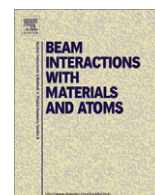
In most cases authors are permitted to post their version of the article (e.g. in Word or Tex form) to their personal website or institutional repository. Authors requiring further information regarding Elsevier's archiving and manuscript policies are encouraged to visit:

<http://www.elsevier.com/copyright>



Contents lists available at ScienceDirect

Nuclear Instruments and Methods in Physics Research B

journal homepage: www.elsevier.com/locate/nimb

Electron transferring from titanium ion irradiated carbon nanotube arrays into vacuum under low applied fields

Jian-hua Deng, Zhao-xia Ping, Rui-ting Zheng, Guo-an Cheng*

Key Laboratory of Beam Technology and Material Modification of Ministry of Education, College of Nuclear Science and Technology, Beijing Normal University, Beijing 100875, People's Republic of China

ARTICLE INFO

Article history:

Received 18 October 2010

Received in revised form 7 March 2011

Available online 17 March 2011

Keywords:

Multiwall carbon nanotube arrays

Titanium ion irradiation

Field emission

Stability behavior

ABSTRACT

Field emission characteristics of carbon nanotube arrays synthesized by thermal chemical vapor deposition on iron ion pre-bombarded silicon substrate are enhanced by titanium ion irradiation. A pronounced degradation of turn-on electric field of $0.305 \text{ V}/\mu\text{m}$ and threshold field, of which the lowest value is only $1.054 \text{ V}/\mu\text{m}$, about $0.482 \text{ V}/\mu\text{m}$ at the dose of $5 \times 10^{16} \text{ ions}/\text{cm}^2$ is as an expression of this enhancement. Scanning electron microscopy, Raman spectroscopy, x-ray photoelectron spectroscopy, Photoelectron spectrometer and transmission electron microscopy are measured for comparison before and after the Ti ion irradiation of the carbon nanotube arrays, and the results reveal that the formation of carbon nanorod/nanotube heterostructure during ion irradiation plays a dominative role in the promotion of the field emission properties. However, high-dose irradiating transaction on carbon nanotube arrays will exert repulsive effects on the field emission characteristics for the introduction of severe structural damage. Additionally, the longtime eminent stability behaviors under high applied fields have provided a possibility for the potential application of field emission flat panel display or electron emitters based on carbon nanotube arrays.

© 2011 Elsevier B.V. All rights reserved.

1. Introduction

Carbon nanotubes (CNTs), which consist of cylindrically closed graphitic sheets, have aroused much speculation as field electron emitters due to their high aspect ratio and chemical stability, high mechanical strength, and superior electrical conductivity [1]. In order to promote field emission (FE) properties of CNTs, numerous technologies have been tried, such as chemical solution post-treatment [2], surface decoration at the tips [3,4] and so on. Ion irradiation, which can be precisely controlled and effectively enhance the field electron emission, has been widely used hitherto. Zhi et al. reported that the field emission characteristics have been greatly improved (from $5.6 \text{ V}/\mu\text{m}$ to $4.2 \text{ V}/\mu\text{m}$ at an emission current density of $5 \text{ mA}/\text{cm}^2$) by hydrogen plasma treatment for the introduction of defects and $C\delta^- - H\delta^+$ dipole layer which can decrease the work function of the emitters [5]. Other reports from Se-Jin Kyung et al. ascribed the drop of turn-on electric field (E_{on} , applied field when the emission current density is $10 \mu\text{A}/\text{cm}^2$) from 1.7 to $0.9 \text{ V}/\mu\text{m}$ to Ar neutral beam treatment which can largely weaken the influence of field screening effect [6,7]. The vertical alignment of CNTs, lower threshold field (E_{th} , applied field when the emission current density is $10 \text{ mA}/\text{cm}^2$, which is the ba-

sic requirement for the application of FPD) and excellent stability behavior of emission current are also indispensable in the attempts to realize the application of field emission display based on carbon nanotube arrays (CNTAs), and substantial researches on these aspects have been carried out in recent years. Reports from Guohai Chen et al. revealed that the emission current density showed no noticeable degradation in 19 hours at $1 \text{ mA}/\text{cm}^2$ by a tip sonication pretreatment which can effectively cut CNTs short and regulate the length of CNTs [8]. Some other reports have provided methods for reducing the E_{on} and E_{th} of emitters by laser treating, element coating or ion irradiation [9–11].

In the present paper, well aligned CNTAs are prepared and followed by an energetic ion bombardment process which involves irradiation by titanium (Ti) ions, and the FE characteristics of the Ti ion irradiated CNTAs have been characterized.

2. Experimental

CNTAs are fabricated by thermal chemical vapor deposition (TCVD) on iron ion pre-bombarded silicon substrate at 750°C . Ammonia (NH_3) pretreatment is processed at a flow of 150 standard cubic centimeter per minute (sccm) for 10 minutes, which has been approved to be beneficial for promoting the activity of catalyst [12]. During CNTs growth, acetylene (C_2H_2) and hydrogen (H_2) with a flow rate of 87:600 are utilized as the carbon source

* Corresponding author. Tel./fax: +86 010 6220 5403.

E-mail address: gacheng@bnu.edu.cn (G.-a. Cheng).

and carrying gas, respectively, and the growth time is 30 minutes. The resulting CNTAs are placed at a whirling specimen holder and irradiated by Ti ions with an average energy of 40 keV at a base pressure of 5×10^{-4} Pa, the incidence angle of the ion beam is about 10 degrees, the irradiation doses vary from 1×10^{16} to $2 \times 10^{17} \text{ cm}^{-2}$ which is determined by the displacement per atom (dpa) calculated by a TRIM simulation program [13].

For FE measurements, a diode configuration with a moveable anode is employed. The prepared CNTAs stuck to a copper cylinder as the cathode against a stainless steel plate as the anode and the space between them is 2.362 mm. FE measurements are carried out in a vacuum chamber with a background pressure of 1×10^{-7} Pa at about 288 K (cold by water). Emission current density versus applied field (J – E) measurements are automatically controlled by a computer with own designed programs. Scanning electron microscopy (SEM, JSM-4800), Raman spectroscopy, x-ray photoelectron spectroscopy (XPS, PHI Quantera SXM), photoelectron spectrometer (AC-2 Riken Keiki) and transmission electron microscopy (TEM, TECNAI F30) are used to determine the structures of CNTs before and after the Ti ion irradiation with different doses.

3. Results and discussion

Energetic ion irradiation on CNTs can cause defect generation, welding, phase change [14–18], and so on, which is dominant depends on the irradiation doses and the incident energy. Fig. 1(a–f) show the SEM pictures of the Ti ion irradiated CNTAs. Fig. 1(a, c, e)

are the side views, and Fig. 1(b, d, f) are the top views corresponding with the irradiation doses of 0, 5×10^{16} and $1 \times 10^{17} \text{ cm}^{-2}$, respectively. It can be found that the CNTs are about 20 μm in length and 40–60 nm in diameter. The well aligned nano-structure, as shown in Fig. 1(a, c, e), reveals that the alignment morphology is not destroyed by the energetic Ti ion irradiation, whereas evident structural evolution can be observed in the top-view images with the increasing irradiation doses. Coalescence of CNTs emerges at the dose of $5 \times 10^{16} \text{ cm}^{-2}$, but most of them still reserve the separate individual morphology, it reveals that the structural change of CNTAs at low irradiation doses is not evident. However, with further increasing the irradiation dose to $1 \times 10^{17} \text{ cm}^{-2}$, the occurrence of net-structure and the disappearance of the separate individual morphology, as shown in Fig. 1(f), declare that severe damage has been brought into CNTAs by the energetic Ti ion irradiation. The TEM image of a single CNT which has been irradiated at the dose of $5 \times 10^{16} \text{ cm}^{-2}$ is shown in Fig. 1(g), it can be seen that the CNT is consisted of two sections: amorphous nanorod at the tip and damage-gradually-decreasing nanotube at the rest. For nanorod at the tip, which has been transformed into amorphous carbon, the layer-structure which usually exists in flawless CNTs can not be identified any more (Fig. 1(j)). For the tubular section, as shown in Fig. 1(h, i), which are corresponding with different parts of the CNT marked by circles in Fig. 1(g), it can be found that the number of damaged graphite layers decreases with the increasing distance from the tip, this is because the incidence angle of Ti ion beam in this experiment is 10 degrees, less damage will be undertaken by those sections away from the tip for the existence of

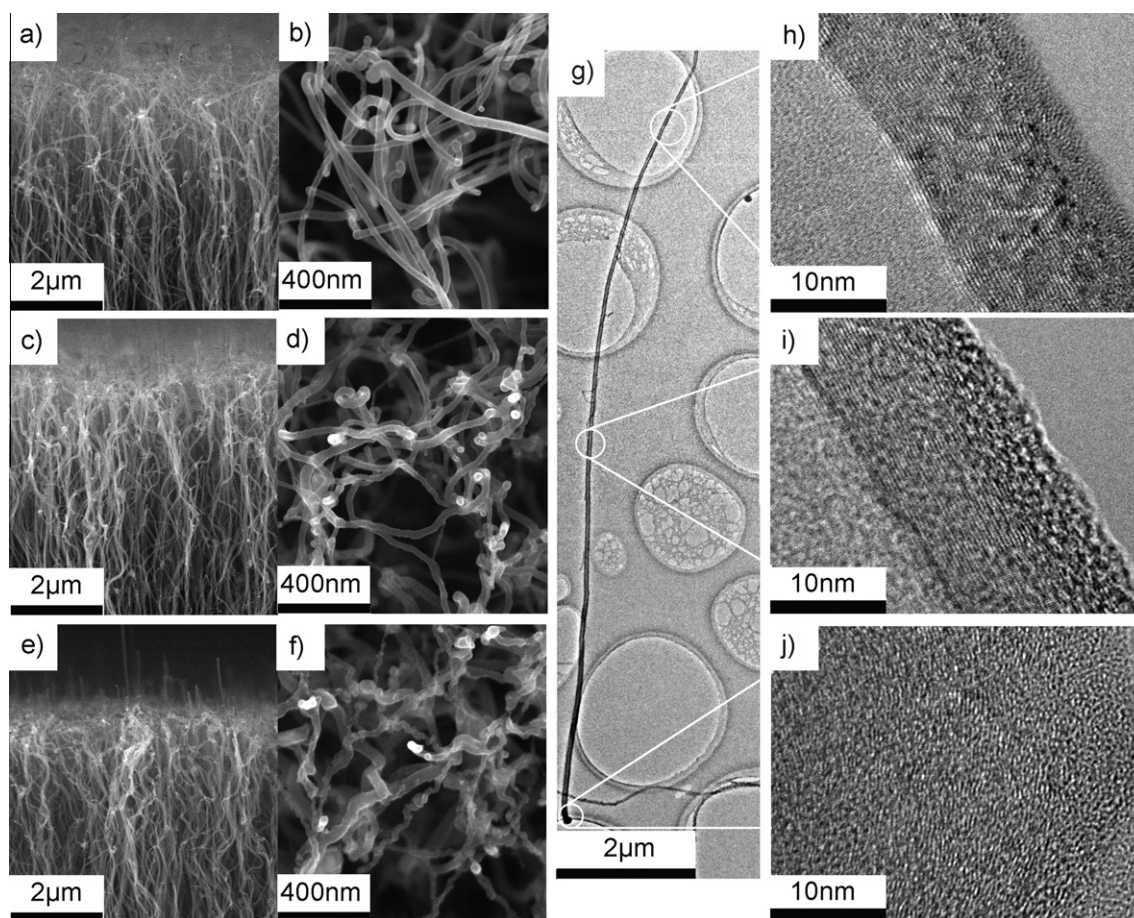


Fig. 1. SEM and TEM pictures of the Ti ion irradiated CNTAs. (a, c, e) are the SEM side views and (b, d, f) are the SEM top views of CNTAs corresponding with the irradiation doses of as-grown, 5×10^{16} and $1 \times 10^{17} \text{ cm}^{-2}$, respectively. (g) shows the low resolution TEM image of a single CNT, of which the irradiation dose is $5 \times 10^{16} \text{ cm}^{-2}$, and (h–j) are high resolution TEM images corresponding with different parts of the CNT which have been marked by three circles in image (g).

mutual shield effect. In short, the occurrence of two kinds of nanostructures, nanorod and nanotube, which are formed in a single one dimensional nano-material demonstrates the formation of carbon nanorod/nanotube (CNR/CNT) heterostructure.

To understand the chemical structure of the CNR/CNT heterostructure, XPS is utilized to characterize the chemical bonds of Ti and C. Fig. 2 shows XPS and Raman spectra of the as-grown and Ti ion irradiated CNTs with different doses. The diversification of the crest value with the increasing irradiation doses has been shown in Fig. 2(a), and the change is not so obvious. Fig. 2(b) shows the decomposed C1s peak of CNTs irradiated at the dose of $5 \times 10^{16} \text{ cm}^{-2}$, the three decomposed peaks centered at 284 eV, 285 eV, and 288 eV are corresponding with graphite carbon [19], diamond-like carbon [20] and organic contaminated carbon [21], respectively. The inset is the percentage change of SP^2 and SP^3 hybridized bond with the increasing irradiation doses, it can be found that the amount of SP^2 hybrid bond (>64%) is far more than SP^3 hybridized bond, and the diversification in both of them is not so obvious which demonstrates that most of the defects induced by ion irradiation among these irradiation doses is in-plane defects (SP^2 -hybridized bond) [22]. Fig. 2(c) shows the XPS spectrum of $\text{Ti}2\text{P}$ peak, and the crest values at 455.3 eV, 458.6 eV, and

464.4 eV demonstrate the formation of TiC [23], TiO_2 ($\text{Ti } 2\text{P}_{3/2}$) and TiO_2 ($\text{Ti } 2\text{P}_{1/2}$) [24], respectively, and it can be found that the amount of TiC is quite small. On the other hand, the formation of TiC compound will decrease the binding energy of C, which will weaken the right-shift of the crest value in C1s peaks induced by the increasing amount of SP^3 hybridized bond (centered at 285 eV), this is in accordance with the not-so-obvious change in the crest value of C1s peaks, as shown in Fig. 2(a). The Raman spectra of the original and Ti ion irradiated CNTs have been shown in Fig. 2(d), the peaks centered at 1342.5 and 1596.0 cm^{-1} are corresponding to the disordered carbon and graphite carbon, respectively [22]. It can be found from the change of sharpness in these Raman peaks that the disordering increases with the irradiation doses, because ion irradiation can introduce defects to CNTs, and the amount of defects, which directly influences on the disordering of CNTs, increases with the irradiation doses when the irradiation dose is not so high.

The FE characteristics have been shown in Fig. 3. Prior to the FE measurements, an aging process [25] is carried out when the emission current density is above 10 mA/cm^2 for 5 hours to weaken the influence of adsorbates induced enhancement of FE characteristics [26] and the deterioration of FE properties for the existence of

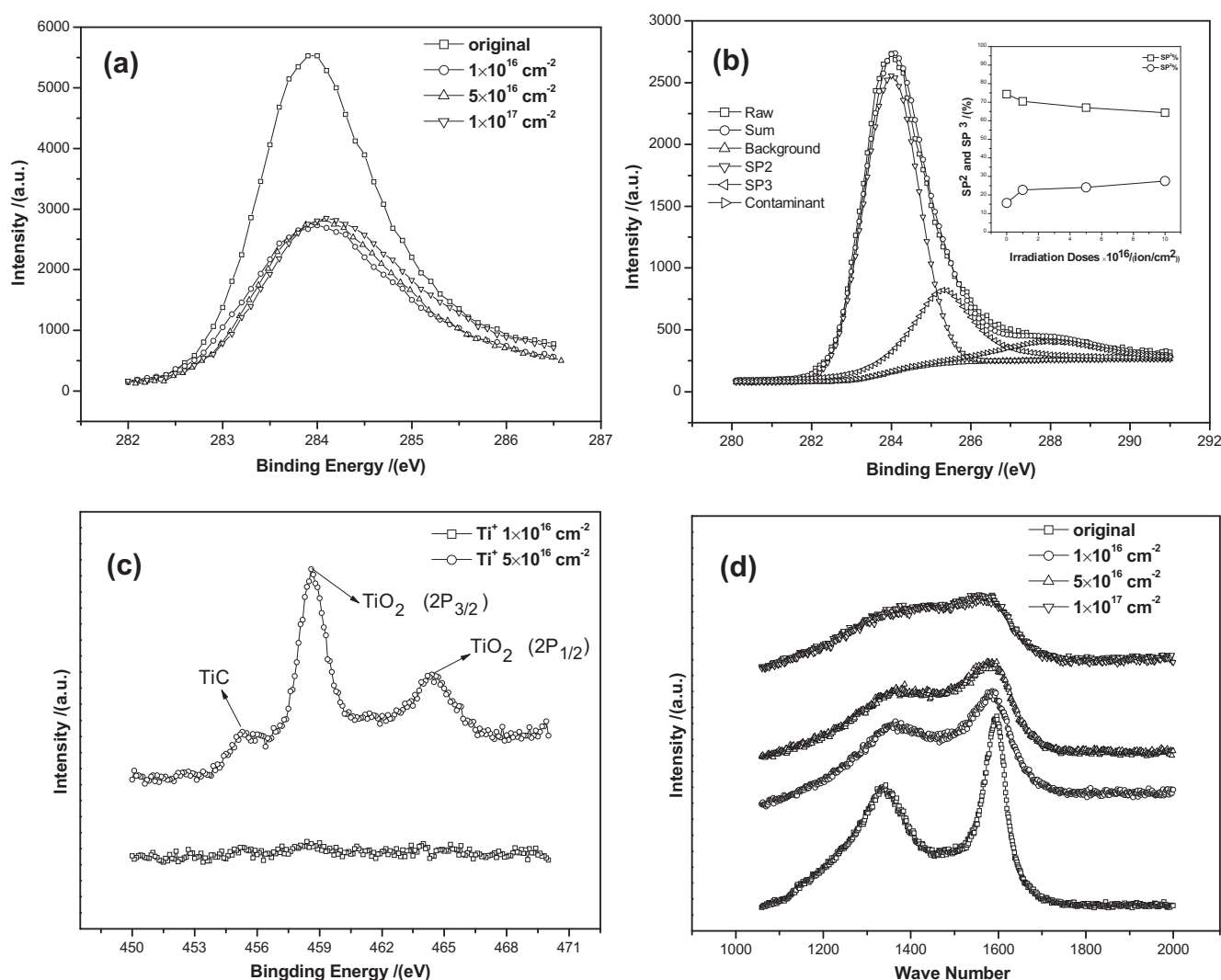


Fig. 2. XPS and Raman spectra of as-grown and Ti ion irradiated CNTs with different doses. (a) Raw C1s peaks of the original and Ti ion irradiated CNTs which reflect the diversification of the crest value with the increasing irradiation doses. (b) C1s peak decomposition of CNTs irradiated at the dose of $5 \times 10^{16} \text{ cm}^{-2}$, the inset is the percentage changes of SP^2 and SP^3 hybridized bond with the increasing irradiation doses. (c) The Raman spectra of Ti 2P peak which demonstrate the formation of TiC compound. (d) Raman spectra of the original and Ti ion irradiated CNTs.

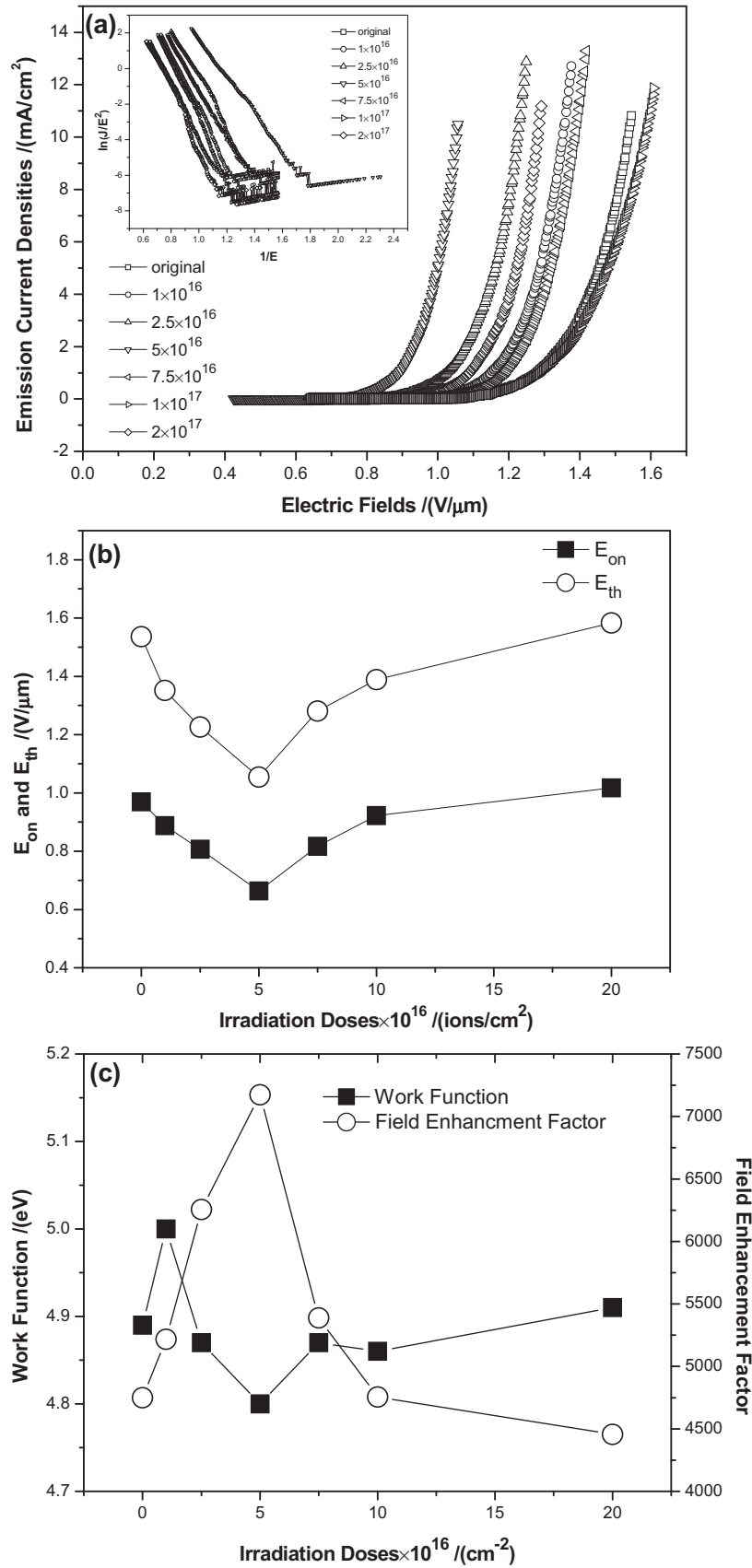


Fig. 3. Field emission characteristics of the original and Ti ion irradiated CNTAs. (a) J - E curves and the inset is the corresponding FN plots. (b) The diversification of E_{on} and E_{th} with the increasing irradiation doses. (c) The change of ϕ and β with different irradiation doses.

Joule-heating induced CNTs burning [25,27]. Fig. 3(a) is given in terms of emission current density (J) and applied field (E), i.e., J – E curves, and the inset is the corresponding FN plots, in which an approximately linear relationship between $\ln(J/E^2)$ and $1/E$ reveals that the electron emission here is aroused by the applied field. Fig. 3(b) shows the diversification of E_{on} and E_{th} . When the irradiation doses are less than $5 \times 10^{16} \text{ cm}^{-2}$, the J – E curves gradually shift to low applied fields with the increasing irradiation doses, which reveals that the FE characteristics have been enhanced by Ti ion irradiation, an evident degradation of E_{on} about $0.305 \text{ V}/\mu\text{m}$ (from 0.969 to $0.664 \text{ V}/\mu\text{m}$) and E_{th} , of which the lowest value is only $1.054 \text{ V}/\mu\text{m}$, about $0.482 \text{ V}/\mu\text{m}$ (from 1.536 to $1.054 \text{ V}/\mu\text{m}$) is as an expression of this enhancement. However, with further increasing the irradiation doses, a shift to high applied field in J – E curves demonstrates that repulsive effects have been brought to FE properties.

The change of work function (ϕ) and field enhancement factor (β), to some extent, can reflect the causes which bring about the change of FE characteristics. With the benefit of photoelectron spectrometer, the work function of each sample is obtained, as shown in Fig. 3(c) (black square). It can be found that the work function of the Ti ion irradiated CNTAs is tending to decrease with the increasing irradiation doses when the dosage is less than $5 \times 10^{16} \text{ cm}^{-2}$, and the lowest work function is obtained (4.80 eV) at the dose of $5 \times 10^{16} \text{ cm}^{-2}$, with one accord, the irradiated CNTAs show the best FE characteristics at this dosage. However, the work function is quite different from the others at the dose of $1 \times 10^{16} \text{ cm}^{-2}$, which is beyond our understanding, hitherto, and it could be an experimental error for it's hard to guarantee that each sample used in this experiment is absolutely the same, or maybe, it's just a measurement error during work function testing. The causes for the decrease of the work function can be elucidated by two mechanisms, one is the promotion of Fermi level induced by the increasing state density of defect during ion irradiation [28], the other is the formation of TiC compound for the work function of TiC is only 3.35 eV [29], but this influence is supposed to be limited for the amount of TiC compound is quite small, as shown in Fig. 2(c). Combining the value of the work function and the FN equation [30], the change of enhancement factor (β) with irradiation doses can be obtained, as shown in Fig. 3 (unfilled circle). The evident diversification of β from 4749 (original) to 7174 ($5 \times 10^{16} \text{ cm}^{-2}$) demonstrates that the microstructure of CNTs has been changed greatly, and the increase of electron transmission traces which are largely related to vacancy-related defects [31] induced by Ti ion irradiation is supposed to be the main cause for this increase of β , so leads to a great improvement (left-shift in J – E curves, Fig. 3 (a)) to FE characteristics of the CNTAs. However, β decreases from 7174 ($5 \times 10^{16} \text{ cm}^{-2}$) to 4457 ($2 \times 10^{17} \text{ cm}^{-2}$) with further increasing the irradiation doses, and this decrease of β , mainly, is also attributed to the change of emission sites which is determined by electron transmission traces. As we know, severe damage can be introduced to CNTs when they are exposed to high dose ion irradiation, and the overly deposited energy will induce the change of microstructure of CNTs, such as CNT–CNT fusion, defects annealing, and so on, which greatly decrease the number of emission sites and deteriorate the FE characteristics of CNTAs. On the other hand, an annealing effect induced by the overly deposited energy will decrease the number of defects which are generated during ion irradiation and lead to a small increase in work function [28], as shown in Fig. 3(c), and this promotion in work function, to some degrees, deteriorates the FE performances of the Ti ion irradiated CNTAs. In a word, the small quantity of TiC in CNTs does exert some but limited influence to the work function of Ti ion irradiated CNTAs, however, the change of microstructures induced by ion irradiation, especially the electron transmission traces, affects the FE characteristics greatly.

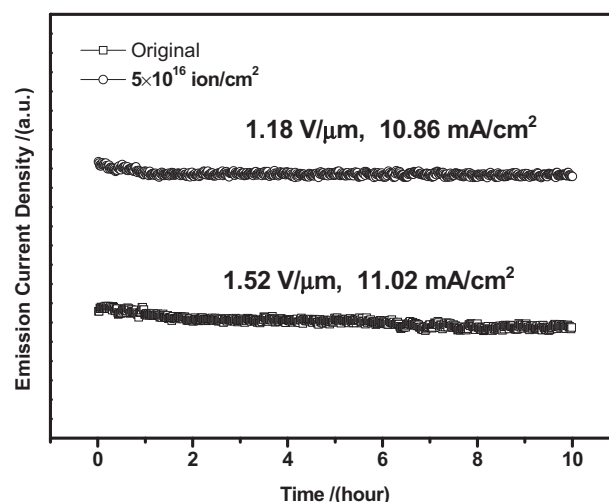


Fig. 4. Stability measurements of the original and Ti ion irradiated CNTs ($5 \times 10^{16} \text{ cm}^{-2}$) above the threshold emission current density ($10 \text{ mA}/\text{cm}^2$).

The longtime eminent stability behavior above threshold emission current density ($10 \text{ mA}/\text{cm}^2$) is essential for the realization of field emission flat panel display based on CNTs. Fig. 4 shows the 10 hours' stability behaviors of the original and Ti ion irradiated CNTs ($5 \times 10^{16} \text{ cm}^{-2}$), of which the mean emission current densities are 11.02 and $10.86 \text{ mA}/\text{cm}^2$, and the corresponding applied fields are 1.52 and $1.18 \text{ V}/\mu\text{m}$, respectively. Two parameters, drop and S_d/V_{mean} , are introduced to characterize the stability of the above two samples. Drop, which is defined as: $(V_{beginning} - V_{last})/V_{mean}$, is a direct reflection of the degradation of emission current density, while S_d/V_{mean} , which is the ratio of standard deviation and the mean value of emission current density, to some extent, reveals the fluctuations in the FE stability measurements. According to the above definition, it can be obtained that the drop and S_d/V_{mean} of the original and Ti ion irradiated CNTs are 3.75% , 1.27% , and 3.41% , 0.58% , respectively. The difference in drop of the two samples is negligible for both of them are aged above $10 \text{ mA}/\text{cm}^2$ for 5 hours, which can largely weaken the degradation of emission current density induced by CNTs burning for the existence of Joule heat during FE measurements. But it's hard for us to ignore the remarkable difference in S_d/V_{mean} , which means that the fluctuations in these two curves are quite different. Because during ion irradiation, some CNTs, especially those with defects or defects clusters, which can be seen in the Raman spectrums (Fig. 2(d)), can be broken off by the energetic ion beam or be annealed by excessive energy deposition, and those CNTs are largely attributed to the degradation of emission current during FE measurements. Hence, the Ti ion irradiated CNTAs will have a more smooth stability curve than the original one during stability measurements. Furthermore, the applied field of the Ti ion irradiated CNTAs is much lower than the original one, which is very important for the application of FPD based on CNTs.

4. Conclusions

Carbon CNR/CNT heterostructure is obtained by energetic Ti ion irradiation. During FE measurements, it has been approved that this heterostructure can greatly enhance the FE characteristics at the irradiation dose of $5 \times 10^{16} \text{ cm}^{-2}$ for the existence of vacancy-related defects, an evident degradation of E_{on} about $0.305 \text{ V}/\mu\text{m}$ (from 0.969 to $0.664 \text{ V}/\mu\text{m}$) and E_{th} , of which the lowest value is only $1.054 \text{ V}/\mu\text{m}$, about $0.482 \text{ V}/\mu\text{m}$ (from 1.536 to $1.054 \text{ V}/\mu\text{m}$) is as an expression of this enhancement. Analysis from XPS shows that TiC compound, which is beneficial for the

decrease of work function of CNTs, has been formed. By using the FN model, the diversification of field enhancement factor (β) is obtained, it can be found that β increases with the irradiation doses from 4749 to 7174 when the dosage is less than $5 \times 10^{16} \text{ cm}^{-2}$, which is derived from the increase of emission sites of CNTs for the increase of vacancy-related defects induced by ion irradiation. However, β decreases with the further increase of irradiation doses, and we attribute this to the decrease of emission sites induced by overly deposited energy. In a word, it's the change of microstructure determined field enhancement factor rather than the diversification of work function that pose a more important influence on the FE characteristics of the Ti ion irradiated CNTAs. The stability testing results reveal that ion irradiation is beneficial for reducing fluctuations in stability measurements, and the longtime eminent stability behavior at threshold field (3.41% drop in 10 hours) provides a possibility for the potential application of flat panel display based on CNTAs.

Acknowledgements

This work is supported by National Basic Research Program of China (No: 2010CB832905), and partially by Key Scientific and Technological Project of Ministry of Education of China (No: 108124).

References

- [1] R.H. Baughman, A.A. Zakhidov, W.A. de Heer, Carbon nanotubes – the route toward applications, *Science* 297 (2002) 787–792.
- [2] S.F. Lee, Y.P. Chang, L.Y. Lee, Enhancement of field emission from carbon nanotubes by post-treatment with a chromium trioxide solution, *New Carbon Mater.* 23 (2008) 104–110.
- [3] C.K. Dong, M.C. Gupta, Influences of the surface reactions on the field emission from multiwall carbon nanotubes, *Appl. Phys. Lett.* 83 (2003) 159–161.
- [4] R.B. Rakhi, K. Sethupathi, S. Ramaprabhu, Electron field emission properties of conducting polymer coated multi walled carbon nanotubes, *Appl. Surf. Sci.* 254 (2008) 6770–6774.
- [5] C.Y. Zhi, X.D. Bai, E.G. Wang, Enhanced field emission from carbon nanotubes by hydrogen plasma treatment, *Appl. Phys. Lett.* 81 (2002) 1690–1692.
- [6] S.J. Kyung, J.B. Park, B.J. Park, J.H. Lee, G.Y. Yeom, Improvement of electron field emission from carbon nanotubes by Ar neutral beam treatment, *Carbon* 46 (2008) 1316–1321.
- [7] J.S. Suh, K.S. Jeong, J.S. Lee, Study of the field-screening effect of highly ordered carbon nanotube arrays, *Appl. Phys. Lett.* 80 (2002) 2392–2394.
- [8] G.H. Chen, D.H. Shin, S. Kim, S. Roth, C.J. Lee, Improved field emission stability of thin multiwalled carbon nanotube emitters, *Nanotechnology* 21 (2010) 015704.
- [9] K.F. Chen, K.C. Chen, Y.C. Jiang, L.Y. Jiang, Y.Y. Chang, M.C. Hsiao, L.H. Chan, Field emission image uniformity improvement by laser treating carbon nanotube powders, *Appl. Phys. Lett.* 88 (2006) 193127.
- [10] F. Jin, Y. Liu, C.M. Day, Barium strontium oxide coated carbon nanotubes as field emitters, *Appl. Phys. Lett.* 90 (2007) 143114.
- [11] Z.C. Ni, A. Ishaq, L. Yan, J.L. Gong, D.Z. Zhu, Enhanced electron field emission of carbon nanotubes by Si ion beam irradiation, *J. Phys. D Appl. Phys.* 42 (2009) 075408.
- [12] H. Zhang, Y.F. Chen, S.S. Kim, Y.S. Lim, Effects of ammonia in catalytic chemical vapor deposition in the synthesis of carbon nanotubes, *Met. Mater. Int.* 14 (2008) 269–273.
- [13] K.F. Chen, J.H. Deng, F. Zhao, G.A. Cheng, R.T. Zheng, Influence of Zn ion implantation on structures and field emission properties of multi-walled carbon nanotube arrays, *Sci. China. Ser. E. Technol. Sci.* 53 (2010) 776–781.
- [14] Z. Osváth, G. Vértesy, L. Tapasztó, F. Wéber, Z.E. Horváth, J. Gyulai, L.P. Biró, Atomically resolved STM images of carbon nanotube defects produced by Ar^+ irradiation, *Phys. Rev. B* 72 (2005) 045429.
- [15] F. Banhart, The formation of a connection between carbon nanotubes in an electron beam, *Nano Lett.* 1 (2001) 329–332.
- [16] M. Zaiser, Y. Lyutovich, F. Banhart, Irradiation-induced transformation of graphite to diamond: A quantitative study, *Phys. Rev. B* 62 (2000) 3058–3064.
- [17] K.F. Chen, J.H. Deng, F. Zhao, G.A. Cheng, R.T. Zheng, Fabrication and properties of Ag-nanoparticles embedded amorphous carbon nanowire/CNT heterostructures, *Nanoscale Res. Lett.* 5 (2010) 1449–1455.
- [18] H.P. Liu, G.A. Cheng, C.L. Liang, R.T. Zheng, Fabrication of silicon carbide nanowires/carbon nanotubes heterojunction arrays by high-flux Si ion implantation, *Nanotechnology* 19 (2008) 245606.
- [19] R. Bertone, A. Casagrande, M. Casarin, A. Glisenti, E. Lanzoni, A. Mirengi, E. Tondello, Tin, Tic and Ti(C, N) film characterization and its relationship to tribological behaviour, *Surf. Interface Anal.* 18 (1992) 525–531.
- [20] P. Sundberg, R. Larsson, B.J. Folkesson, On the core electron binding energy of carbon and the effective charge of the carbon atom, *Electron Spectrosc.* 46 (1988) 19–29.
- [21] D. Rats, L. Vandenbulcke, R. Herbin, R. Benoit, R. Erre, V. Serin, J. Sevely, Characterization of diamond films deposited on titanium and its alloys, *Thin Solid Films* 270 (1995) 177–183.
- [22] T. Tanabe, Radiation damage of graphite – degradation of material parameters and defect structures, *Phys. Scripta T64* (1996) 7–16.
- [23] L. Ramquist, K. Hamrin, G. Johansson, A. Fahlman, C. Nordling, Charge transfer in transition metal carbides and related compounds studied by ESCA, *J. Phys. Chem. Solids* 30 (1969) 1835–1847.
- [24] G. Hopfengartner, D. Borgmann, I. Rademacher, G. Wedler, E. Hums, G.W. Spitznagel, XPS studies of oxidic model catalysts: Internal standards and oxidation numbers, *J. Electron Spectrosc.* 63 (1993) 91–116.
- [25] W.H. Liu, X. Li, C.C. Zhu, Improving the emission characteristics of a carbon nanotube cathode in an aging process, *Ultramicroscopy* 107 (2007) 833–837.
- [26] C. Li, G.J. Fang, X.X. Yang, N.S. Liu, Y.P. Liu, X. Effect of adsorbates on field emission from flame-synthesized carbon nanotubes, *Z. Zhao, J. Phys. D Appl. Phys.* 41 (2008) 195401.
- [27] K.A. Dean, T.P. Burgin, B.R. Chalamal, Evaporation of carbon nanotubes during electron field emission, *Appl. Phys. Lett.* 79 (2001) 1873–1875.
- [28] G. Kim, B.W. Jeong, J. Ihm, Deep levels in the band gap of the carbon nanotube with vacancy-related defects, *Appl. Phys. Lett.* 88 (2006) 193107.
- [29] D.A. Da, Vacuum design manual, third ed., National Defence Industry Press, Lanzhou, China, 2004. pp. 1620–1621.
- [30] R.H. Fowler, L.P. Nordheim, Electron emission in intense electric fields, *Roy. Soc. Lond. A-Conta.* 119 (1928) 173–181.
- [31] G. Wei, Emission property of carbon nanotube with defects, *Appl. Phys. Lett.* 89 (2006) 143111.